1 **Large leaf hydraulic safety margins limit the risk of drought-induced leaf hydraulic**

2 **dysfunction in Neotropical rainforest canopy tree species**

3

4 Camille Ziegler[1,2,†,*] (ORCID: 0000-0002-0855-1347), Sébastien Levionnois[1,3,†,*] (ORCID:

5 0000-0002-7217-9762), Damien Bonal[2] (ORCID: 0000-0001-9602-8603), Patrick Heuret[1,3]

6 (ORCID: 0000-0002-7956-0451), Clément Stahl[1] (ORCID: 0000-0001-5411-1169), Sabrina

7 Coste[1] (ORCID: 0000-0003-3948-4375)

8

9 [†]These authors contributed equally to this work

10 [1]UMR EcoFoG, AgroParisTech, CIRAD, CNRS, INRAE, Université des Antilles, Université

11 de Guyane, 97310 Kourou, France.

12 [2]Université de Lorraine, AgroParisTech, INRAE, UMR SILVA, 54000 Nancy, France.

13 [3]AMAP, Univ. Montpellier, CIRAD, CNRS, INRAE, IRD, 34000 Montpellier, France.

14

15 *Authors for correspondence:

16 Camille Ziegler, PhD

17 Email: camille.ziegler9@gmail.com

18 Sébastien Levionnois, PhD

19 Email: sebastien.levionnois.pro@gmail.com

ABSTRACT

(1) The sequence of key water potential thresholds from the onset of water stress to mortality, and the timing of stomatal closure with regard to leaf xylem embolism formation are essential to characterizing plant adaptive strategies to drought. This constitutes a critical knowledge gap for tropical rainforest species, which may be less vulnerable to drought than previously thought.

(2) We recorded key leaf and stem water potential thresholds, leaf hydraulic safety margins (HSM_{leaf}), leaf stomatal safety margins (SSM_{leaf}) and estimated native embolism levels during a normal-intensity dry season across 18 Neotropical rainforest tree species. We also solved a sequence of key water potential thresholds. Additionally, we provide a cross-biome analysis of leaf stomatal safety margins encompassing 97 species from four major biomes based on a literature survey.

(3) In the studied rainforest species, leaf turgor loss point, used as a surrogate for stomatal closure, typically occurred before the onset of leaf xylem embolism. Most species exhibited positive HSM_{leaf} and SSM_{leaf}, with contrasting values across species and nearly absent embolism levels during the dry season irrespective of the experienced midday leaf water potentials. Our results point out that leaf xylem embolism is not routine for Neotropical rainforest tree species.

(4) Based on our proposal of the water potential sequence for tropical rainforest trees, we argue that leaf xylem embolism is a rare event for these species. This was supported by the literature survey, indicating that across biomes, most woody species have rather large SSM_{leaf} and that leaves of tropical rainforest trees are not necessarily more vulnerable than in other biomes. However, we found evidence that some tropical rainforest species may be more vulnerable than others to ongoing climate change. Our data provide an opportunity to parametrize tree-based or land-surface models for tropical rainforests.

Keywords: drought, embolism, hydraulic, optical visualization, safety margin, tropical, turgor loss point, xylem

1 INTRODUCTION

The link between extreme drought events and forest mortality is established at the global scale (Brodribb, Powers, Cochard, & Choat, 2020; Hartmann et al., 2022). However, the increasing frequency of drought events makes a better understanding of the physiological response of trees to drought urgent, and this lack of understanding limits our ability to identify the mechanisms underlying ongoing shifts in tree communities (Esquivel-Muelbert et al., 2019). In this perspective, recent progress in understanding tree mortality and identifying key drought-resistance traits has made it possible to incorporate plant hydraulics in several process-based land surface models (Choat et al., 2018; Eller et al. 2020; Fisher & Koven, 2020; Li et al. 2021). Still, determining the sequence of key water potential thresholds during dehydration, from the onset of water stress to mortality, and the relationships among drought resistance traits remains an important challenge (Bartlett, Klein, Jansen, Choat, & Sack, 2016; Trueba et al., 2019; Yao et al., 2021). Indeed, the sequence of water potential thresholds directly reflects whole-plant drought-survival, and the cross-species variability in these thresholds is informative on the diversity of plant adaptive strategies to drought (Martin-StPaul, Delzon, & Cochard, 2017; Blackman et al., 2019).

In the field, the stem xylem hydraulic safety margin, defined as the difference between the minimum seasonal midday water potential (P_{min}; MPa) and the water potential causing a 50% loss in stem xylem conductivity ($P_{50,stem}$; MPa), reflects the strength of the hydraulic system compared to the experienced hydric stress, and has been shown to predict drought-induced plant mortality at the global scale (Anderegg et al., 2016). Although plant water availability and other water-use traits may matter, the variability in the hydraulic safety margin depends mostly on $P_{50,stem}$ as well as on the point of stomatal closure. Past this point plant water-loss and excessive drops in water potential are drastically reduced, and this in turn controls the variability in P_{min} (Sperry, Hacke, Oren, & Comstock, 2002). Stomatal closure has also been shown to be mechanistically related to a loss in leaf-cell turgor (Brodribb & Holbrook, 2003; Brodribb, Holbrook, Edwards, & Gutierrez, 2003; Rodriguez-Dominguez et al., 2016), and there is often a solid correspondence between these two traits (Bartlett et al., 2016; Martin-StPaul et al., 2017). This is due to the sensitivity of guard cells controlling stomatal aperture to changes in turgor or volume of neighboring cells (Buckley, 2019). Subsequently, leaf turgor loss point (P_{tlp}) has been used as a surrogate for stomatal closure (Martin-StPaul et al., 2017), and has been shown to correlate with dry-season declines in tree sapflux for tropical rainforest tree species (Maréchaux et al., 2018) while varying broadly across species and major biomes

3

82   (Zhu et al., 2018). Stomatal closure is known to precede and delay embolism formation in

83   stem xylem (Martin-StPaul et al., 2017; Mencuccini et al., 2015). Additionally, leaf-stem

84   vulnerability segmentation, when leaf xylem is more vulnerable to drought-induced

85   embolism than stem xylem, has been reported for some species (Hochberg et al., 2016;

86   Klepsch et al., 2018; Levionnois et al., 2020; Li et al., 2020; Rodriguez-Dominguez, Carins

87   Murphy, Lucani, & Brodribb, 2018; Skelton, Brodribb, & Choat, 2017; Skelton et al., 2018;

88   Smith-Martin, Skelton, Johnson, Lucani, & Brodribb, 2020) and has been suggested as a

89   mechanisms that slows down plant desiccation, since leaf xylem embolism allows a drastic

90   reduction of leaf evaporative surface area (Blackman, Li, et al., 2019; Levionnois et al.,

91   2021).

92   Therefore, the water potential causing a 50% loss in leaf xylem conductance ($P_{50,leaf}$;

93   MPa) is a crucial threshold, especially for species showing leaf-stem vulnerability

94   segmentation, with leaves being more vulnerable to the loss of conductance than stems

95   ($P_{50,leaf} > P_{50,stem}$). Indeed, the magnitudes of the leaf hydraulic safety margin (P_{min} - $P_{50,leaf}$;

96   HSM_{leaf}) and of the leaf stomatal safety margin (P_{tlp} - $P_{50,leaf}$; SSM_{leaf}) partly determine the

97   timing of the loss in leaf xylem hydraulic conductance, and consequently influence whole-

98   plant desiccation time (Blackman, Li, et al., 2019; Levionnois et al., 2021). Drastic losses of

99   leaf xylem conductance may strongly impact tree assimilation and productivity (Brodribb et

100   al., 2021; Scoffoni et al., 2016), which is detrimental since re-growing stem xylem is an

101   important post-drought recovery mechanism (Brodribb et al., 2021; Creek, Blackman,

102   Brodribb, Choat, & Tissue, 2018; Gauthey et al., 2022). Recently, it has been established

103   that stem xylem conductivity loss caused by embolism is irreversible in the absence of xylem

104   vessel refilling through positive root pressure (Schenk, Jansen, & Hölttä, 2020), and this may

105   also be the case for leaves (Johnson, Jordan, & Brodribb, 2018). For tall trees experiencing

106   strong water potential gradients, xylem refilling is therefore unlikely (Schenk et al., 2020),

107   highlighting the catastrophic consequences of xylem embolism.

108   Following the early work of Nardini and Salleo (2000), several studies have supported

109   the idea that leaf xylem "embolism" may be a trigger for the down-regulation of stomatal

110   conductance during drought (Brodribb & Holbrook, 2003; Johnson, Woodruff, McCulloh, &

111   Meinzer, 2009; Lo Gullo, Nardini, Trifilò, & Salleo, 2003; Nardini, Tyree, & Salleo, 2001;

112   Savi et al., 2016; Torres-Ruiz, Diaz-Espejo, Perez-Martin, & Hernandez-Santana, 2015).

113   Yet, these studies integrated the extra-xylary pathway, which is more sensitive to declining leaf

114   water potential and itself constitutes a large fraction of whole-leaf conductance loss (Ocheltree,

115   Gleason, Cao, & Jiang, 2020; Scoffoni, Albuquerque, Brodersen, Townes, John, Bartlett, et al.,

116   2017). Accordingly, most HSM_{leaf} and SSM_{leaf} reported in global meta-analyses integrate the

117   losses in leaf conductance from both xylary and extra-xylary pathways (Bartlett et al., 2016;

118   Scoffoni, Sack, & Ort, 2017; Yan, Ni, Cao, & Zhu, 2020); this has hampered our understanding

119   of the timing of leaf xylem embolism formation with regard to stomatal response to drought.

120   However, growing evidence suggests that stomatal closure, either measured directly or

121   estimated with P_{tlp}, rather occurs before embolism formation in the leaf xylem, and that species

122   with larger SSM_{leaf} delay the irreversible loss of hydraulic conductance (Cardoso, Brodribb,

123   Lucani, DaMatta, & McAdam, 2018; Creek et al., 2020; Dayer et al., 2020; Hochberg et al.,

124   2017; Li et al., 2019; Manzi et al., 2022; Skelton et al., 2018, 2021; Sorek et al., 2021) and

125   suffer less from mortality during record drought events (Powers et al., 2020). These studies

126   were based on direct observations of leaf vulnerability to embolism, which should guarantee

127   less ambiguous conclusions on the timing of stomatal closure relative to leaf xylem embolism,

128   and eventually make it possible to identify a complete water potential sequence. In this effort,

129   Manzi et al., (2022) showed that P_{tlp} preceded leaf xylem embolism in saplings of five rainforest

130   tree species grown in controlled conditions. This investigation should be extended to mature

131   trees and particularly on the same individuals, and to locally coexisting tropical rainforest

132   canopy tree species. Whether tree leaves often undergo xylem embolism during drought *in*

133   *natura* also remains unknown.

134   Rainforest species are assumed to show lower interspecific variation and higher

135   vulnerability to drought than species from drier biomes (Choat et al., 2012). However, recent

136   studies have found contrasting hydraulic and stomatal safety margins within tree communities,

137   thereby challenging this assumption (Barros et al., 2019; Ziegler et al., 2019; Fontes et al., 2020;

138   Vargas et al., 2021). Yet, for tropical rainforests, hydraulic and drought resistance studies

139   cover only a limited range of species relative to the strong specific diversity (Oliveira et al.,

140   2021). The physiological response of trees is a major uncertainty in global vegetation models,

141   and this knowledge gap presently hampers robust predictions on the fate of tropical

142   rainforests (Huntingford et al., 2013; Pugh et al., 2020). It has been demonstrated that most

143   tree species maintain large stem hydraulic safety margins due to a combination of low

144   vulnerability to embolism and timely stomatal closure (Ziegler et al., 2019). However, the

145   existence of species showing vulnerability segmentation (Levionnois et al., 2020) questions the

146   magnitude of the interspecific variations in leaf hydraulic safety margins and its ecological

consequences in the relatively moist and thermally stable tropical climate, with regard to the broad cross-species differences found for drier biomes (Creek et al., 2020).

In this study, we tested the coordination between leaf xylem vulnerability to embolism, leaf turgor loss point (used as a surrogate for the water potential causing stomatal closure), and the experienced dry season midday leaf water potential for 18 tropical rainforest canopy tree species. Furthermore, we resolved an extensive sequence of physiological thresholds during dehydration for rainforest canopy tree species. With regard to the broad phylogenetic diversity of tropical rainforests, we aimed to evaluate whether tree species show a functional convergence in terms of hydraulic safety margins or whether their drought-response strategies are divergent. We retrieved hydraulic trait data from published work conducted at the same site. We built vulnerability curves (VC) to quantify xylem vulnerability to drought-induced embolism which has been measured in leaves with the optical vulnerability (OV) method and in stems with the flow-centrifugation technique. Finally, to compare data on leaf stomatal safety margins gathered for tropical rainforest tree species with species from other biomes, we performed a literature survey of the studies that also used the OV method to measure leaf xylem vulnerability to embolism. We specifically addressed the following questions:

(i) Does leaf turgor loss point occur before embolism formation in the leaf xylem, and do leaves develop xylem embolism during the dry season in co-occurring Neotropical tree species?

(ii) What is the sequence and interspecific variability in key water potential thresholds during dehydration for Neotropical canopy tree species?

(iii) Are tropical rainforest tree species more subject to leaf hydraulic dysfunction than species from other biomes?

2 MATERIALS AND METHODS

2.1 *Study site, species, and design*

The experiment was conducted in French Guiana at the Paracou experimental station (https://paracou.cirad.fr/website; 5°16'26''N, 52°55'26''W), in a lowland tropical rainforest (Gourlet-Fleury, Guehl, & Laroussinie, 2004). The warm, wet tropical climate of French Guiana is highly seasonal due to the North-South movement of the Inter-Tropical Convergence Zone. Mean (± SE) annual air temperature is 25.7 °C ± 0.1°C and mean annual precipitation is 3,102 mm ± 70 mm (data between 2004 and 2014; Aguilos et al., 2019). There is a dry season lasting from mid-August to mid-November, during which rainfall is < 100 mm month^{-1}.

180   The dataset presented in this study results from the pooled datasets of Ziegler et al.,
181   (2019) and Levionnois et al., (2020), who conducted their studies on the same trees during
182   common measurement campaigns and measured stem and leaf xylem vulnerability to
183   embolism, leaf turgor loss point and leaf midday water potential. The studied species covered
184   a broad phylogenetic diversity such that the main clades of the flowering plants were
185   represented, i.e. magnoliids, rosids, and asterids. We sampled dominant canopy trees growing
186   within a 1 km radius on plateaus or moderate slopes (i.e. *terra firme*), at the exception of *G.*
187   *hexapetala*, an understorey species (Table 1). A total of 50 trees from 18 different species were
188   selected, with three trees per species for 14 species, and two trees per species for four species
189   (*B. prouacensis*, *C. sanguinolentum*, *L. poiteauii, Q. rosea*).
190
191   2.2 *Dry season midday leaf water potential*
192   Midday leaf water potential (P_{md}; MPa) was measured on sun-exposed canopy branches with a
193   pressure chamber (Model 1505D, PMS, USA) between 11:00 and 14:00 on clear sunny days
194   with a high vapor pressure deficit (VPD = 1.27 ± 0.23 kPa) in early October during the 2018
195   dry season when relative extractable soil water (REW, unitless) was low (REW = 0.23 ± 0.01;
196   Ziegler *et al.*, 2019). Environmental conditions during these measurements were typical of an
197   average intensity dry season, according to 40 years of available REW data (Ziegler et al., 2019).
198   The detailed method and data for each species are available and discussed in Ziegler et al.,
199   (2019).
200
201   2.3 *Leaf turgor loss point and water potential at stomatal closure*
202   The water potential at stomatal closure is generally determined through stomatal sensitivity
203   curves, which describe the loss of stomatal conductance as leaf water potential decreases
204   (Brodribb & Holbrook, 2003; Creek et al., 2020). However, the necessary measurements for
205   this approach are long and laborious, especially for tall canopy trees. Following several studies
206   supporting a mechanistic links between leaf-cell turgor loss and stomatal closure, (Bartlett et
207   al., 2016; Brodribb & Holbrook, 2003; Brodribb, Holbrook, Edwards, & Gutierrez, 2003;
208   Buckley, 2019; Hochberg, Rockwell, Holbrook, & Cochard, 2018; Martin-StPaul et al., 2017;
209   Rodriguez-Dominguez et al., 2016), we used leaf turgor loss point (P_{tlp}) as a surrogate for the
210   water potential at stomatal closure. We retrieved P_{tlp} data measured with a vapor pressure
211   osmometer (VAPRO 5520, Wescor, Logan, UT, USA; Bartlett et al., 2012) for previous work
212   during the 2018 dry season on sun-exposed canopy branches of the same individual trees that

213   had been measured for P_{md} and vulnerability to leaf and stem xylem embolism (Ziegler et al.,

214   2019). P_{tlp} was not available for only one species: *Q. rosea*. The data and the detailed method

215   for each species are available and discussed in Ziegler et al., (2019).

216

217   2.4 *Leaf and stem xylem vulnerability to embolism*

218   Professional tree climbers sampled 2-3-m-long sun-exposed canopy branches during the wet

219   season. For leaf xylem vulnerability to embolism, field sampling was carried out between

220   November 2018 and March 2019. Generally, we sampled three trees per sampling day, in the

221   morning before solar midday in order to avoid too negative leaf water potentials. One one-

222   meter-long canopy branch with ~20-50 leaves was sampled per tree to monitor water potentials.

223   To measure leaf xylem vulnerability to embolism, we used the optical light transmission method

224   (Brodribb, Bienaime, & Marmottant, 2016; Brodribb, Skelton, et al., 2016) with a high-

225   resolution scanner (Epson Perfection V800; Epson America Inc., Long Beach, CA, USA) and

226   stem psychrometers (ICT International, Armidale, NSW, Australia). To measure stem xylem

227   vulnerability to embolism, neighboring canopy branches of the same individual trees had

228   previously been sampled between January and July 2017. Measurements were realized with the

229   flow-centrifugation technique in a large 1-m diameter rotor designed to process long-vesseled

230   species (Burlett et al., 2022). We also measured maximum vessel length (MVL) on neighboring

231   branches (see data in Ziegler et al., 2019). To avoid open-vessel artefacts, we selected smaller-

232   diameter branches for species with MVL close to 1 m, since vessel length has been shown to

233   increase with branch diameter (Jacobsen, Pratt, Tobin, Hacke, & Ewers, 2012).

234   Vulnerability curves were fitted with a sigmoid curve (Pammenter & Van der Willigen,

235   1998) with the 'fitplc' function of the *fitplc* package in R (Duursma & Choat, 2017). From these

236   vulnerability curves, we then quantified leaf and stem xylem vulnerability to embolism as the

237   water potential inducing 12%, 50% and 88% loss of conductance in the leaves and stems

238   (respectively $P_{12,leaf}$, $P_{50,leaf}$, $P_{88,leaf}$, $P_{12,stem}$, $P_{50,stem}$ and $P_{88,stem}$; MPa). P_{50} is widely considered

239   to represent species xylem resistance to hydraulic dysfunction and is typically used for cross-

240   species comparison. P_{12} is a more conservative threshold, considered to represent the water

241   potential associated with initial air entry causing incipient damage to the hydraulic system

242   (Meinzer, Johnson, Lachenbruch, McCulloh, & Woodruff, 2009). In stems, P_{88} represents the

243   mean water potential causing irreversible hydraulic damage leading to canopy dieback in

244   angiosperms (Urli et al., 2013). The slope of the leaf and stem vulnerability curves (a_x; %MPa$^-$

245   ^{1}), describing the speed at which embolism affects leaf and stem xylem, was also extracted from

vulnerability curves. For details on the methods and data for each species of this study we refer the reader to Ziegler et al., (2019) and Levionnois et al., (2020).

2.5 *Leaf safety margins and percentage loss in leaf xylem hydraulic conductance*

Leaf stomatal safety margins (P_{12} SSM_{leaf}; MPa) were calculated such that: P_{12} SSM_{leaf} = P_{tlp} - $P_{12,leaf}$, and leaf hydraulic safety margins (HSM_{leaf}; MPa) were calculated such that: HSM_{leaf} = P_{md} - $P_{12,leaf}$. Safety margins were calculated for individual trees, then averaged at the species level. The dry season percentage loss in leaf xylem hydraulic conductance (PLC) was estimated at the individual leaf level through vulnerability curves as in Cochard 2006:

$$PLC = \frac{100}{\left[1 + \exp\left(\frac{a_x}{25} \times (P_{md} - P_{50,leaf})\right)\right]}$$

with P_{md} (MPa), representing the dry season midday leaf water potential, $P_{50,leaf}$ the leaf water potential inducing 50% loss of leaf xylem conductance and a_x (%MPa^{-1}) the slope of the vulnerability curve at $P_{50,leaf}$.

2.6 *Literature survey*

To minimize uncertainties related to differing techniques to measure leaf xylem vulnerability to embolism (Scoffoni, Sack & Ort, 2017), we included only the species measured with the optical vulnerability method (Brodribb, Bienaime, & Marmottant, 2016; Brodribb, Skelton, et al., 2016), in the literature survey for the present study. This allowed us to compare of the vulnerability of leaf xylem only, not of the whole leaf, which includes the extra-xylary pathway, taken into account when other techniques are used. From 14 recently published studies (from 2016 to 2022), we compiled data for 97 species (mostly trees) belonging to Mediterranean and dry forests (MED; n = 13), temperate forests (TEMP; n = 20), tropical dry forests (TDF; n = 44) and tropical rainforests (TRF; n = 20; this study and Manzi et al., 2022). We extracted i) leaf xylem vulnerability to embolism quantified as $P_{50,leaf}$, which was commonly reported, and ii) the water potential associated with stomatal closure (P_{close}; MPa), determined either from turgor loss point (P_{tlp}; n = 96 species) or, when P_{tlp} was not available, from gas-exchange measurements (n = 3 species; See Supplementary Table S1 for species details). From the literature survey, we computed the leaf stomatal safety margin for each species as $P_{close} - P_{50,leaf}$ (P_{50} SSM_{leaf}; MPa). For some species, data were available from several studies and, in this case, were averaged to obtain a mean trait value per species. Information on the species' biome was also gathered.

9

279   2.7 *Statistical analyses*

280   All statistical analyses were performed with the R software (R Core Team, 2018). To address

281   question (i) as accurately as possible while accounting for inter-tree variation, we included in

282   the analysis only trees for which all the selected traits (i.e. $P_{12,leaf}$, $P_{50,leaf}$, P_{tlp} and P_{md}) were

283   available. For correlations between traits, we used Pearson or Spearman correlation analyses

284   depending on the normality of the distribution (Shapiro-Wilk test; $\alpha = 0.05$). To address

285   question (ii), we were interested in the most robust mean trait value estimate at the species level.

286   We therefore included the maximum number of measured trees per species for each trait

287   according to data from Ziegler et al., (2019) and Levionnois et al., (2020). To address question

288   (iii), after testing for the normality of the distribution (Shapiro-Wilk test; $\alpha = 0.05$), differences

289   in leaf hydraulic safety margin across biomes were tested with a Kruskall-Wallis test.

290

291   **3 RESULTS**

292   3.1 *Leaf safety margins and xylem embolism during drought*

293   Across the studied rainforest tree species, leaf xylem vulnerability to embolism ($P_{50,leaf}$) varied

294   from -4.6 to -2.3 MPa, and $P_{12,leaf}$ varied from -4.1 to -1.4 MPa. By contrast, the magnitude of

295   the interspecific variation in the leaf water potential at stomatal closure, quantified as P_{tlp}, varied

296   much less, from -2.3 to -1.3 MPa (Table 1). $P_{12,leaf}$ and $P_{50,leaf}$ were unrelated to P_{tlp} (Fig. 1a,b).

297   Moreover, on average, $P_{12,leaf}$ was more negative than P_{tlp} for all but one species (*L. poiteauii*),

298   for which P_{tlp} was less negative than $P_{12,leaf}$ (Fig. 1a), and $P_{50,leaf}$ was more negative than P_{tlp} for

299   all species (Fig. 1b). In the dry season of 2018, P_{md} varied from -2.4 to -0.9 MPa across species

300   and was less negative than $P_{12,leaf}$ for all but one species (*L. poiteauii*; Fig. 1c) and less negative

301   than $P_{50,leaf}$ for all species (Fig. 1d).

302   As a consequence of the relatively small range of variation of P_{tlp}, the P_{12} stomatal safety margin

303   (P_{12} SSM_{leaf}) varied strongly, ranging from -0.9 to 2.1 MPa, mainly according to variation in

304    $P_{12,leaf}$ (Fig. 2a,b). Similarly, P_{50} SSM_{leaf} was also strongly related to $P_{50,leaf}$ (Fig. S1a and S1b).

305   The P_{12} hydraulic safety margin (P_{12} HSM_{leaf}) also varied strongly, ranging from -0.4 to 3.1

306   MPa and varied according to variation in $P_{12,leaf}$, rather than to variation in P_{md} (Fig. 2c,d).

307   Similarly, P_{50} HSM_{leaf} was also strongly related to $P_{50,leaf}$ (Fig. S1c,d). In 2018, three out of 18

308   species with narrow HSM_{leaf} developed some leaf xylem embolism (PLC_{2018}; *C.*

309   *sanguinolentum*, 47%; *D. guianensis*, 25%; *L. poiteauii*, 28%).

310

311   3.2 *Sequence of water potential thresholds*

312   By summarizing the main findings of Ziegler et al., (2019), of Levionnois et al., (2020) and of
313   the present study, we determined a sequence of water potential thresholds, from stomatal
314   closure, estimated with P_{tlp}, to increasing levels of dehydration-induced leaf and stem declines
315   in xylem hydraulic conductance (Fig. 3). Leaf water potential at turgor loss point was reached
316   before the onset of leaf ($P_{12,leaf}$) and stem ($P_{12,stem}$) xylem embolism, both of which considerably
317   overlapped. They were followed sequentially by $P_{50,leaf}$, $P_{88,leaf}$, $P_{50,stem}$ and $P_{88,stem}$. Leaves had
318   lower interspecific variation in xylem vulnerability to embolism than did supporting stems, and
319   steeper vulnerability curve slopes; $P_{50,leaf}$ was less negative than $P_{50,stem}$ in eight out of 18 species
320   (Table S2, but see Levionnois et al., 2020 and Ziegler et al., 2019). Placing P_{md} on this sequence
321   showed that a large proportion of species did not reach P_{tlp}, $P_{12,leaf}$ or $P_{12,stem}$ during a normal-
322   intensity dry season.
323
324   3.3 *Literature survey*
325   According to our literature survey, $P_{50,leaf}$ showed a high cross-biome interspecific variation. It
326   varied from -4.6 to -2.3 MPa for tropical rainforests, from -11.0 to -1.4 MPa for tropical dry
327   forests, from -6.3 to -3.0 MPa for Mediterranean and dry forests and from -5.7 to -1.7 MPa for
328   temperate forests. The range of water potential values at which the same species reached P_{close}
329   showed a narrower variation. It varied from -2.3 to -1.5 MPa for tropical rainforests, from –4.2
330   to -1.3 MPa for tropical dry forests, from -3.3 to -1.8 MPa for Mediterranean and dry forests
331   and from -2.7 to -1.1 MPa for temperate forests. As a result, P_{50} SSM_{leaf} varied from 0.5 to 2.9
332   MPa for tropical rainforests, from –0.7 to -6.8 MPa for tropical dry forests, from 0.6 to 4.1 MPa
333   for Mediterranean and dry forests and from 0.4 to 3.8 MPa for temperate forests. There were
334   no cross-biome differences in P_{50} SSM_{leaf} (P = 0.58; Fig. 4). We found broad within-biome
335   variations with a mean ± SD of 1.6 ± 0.7 MPa for tropical rainforests, 2.1 ± 1.6 MPa for tropical
336   dry forests, 2.2 ± 1.1 MPa for Mediterranean and dry forests and 1.8 ± 0.8 MPa for temperate
337   forests. Across biomes, most species (~97%) showed a positive P_{50} SSM_{leaf} (P_{tlp} - $P_{50,leaf}$ > 0).
338
339   **4 DISCUSSION**
340   Our results indicate that most of the sampled Neotropical rainforest tree species avoid
341   substantial leaf xylem embolism thanks to large leaf hydraulic and leaf stomatal safety margins.
342   Our data on the interspecific variation in P_{12} SSM_{leaf} supports the hypothesis that cell turgor
343   loss, and subsequent stomatal closure, occur before the onset of leaf xylem embolism, thereby
344   protecting leaf xylem during drought. The broad interspecific variability in hydraulic safety

11

345 margin suggests that co-occurring species might respond differently to the increasing frequency

346 of drought severity. Finally, we show that tropical rainforest tree species may not be at higher

347 risk of leaf xylem embolism in comparison to other biomes.

348

349 4.1 *Leaf turgor loss precedes leaf xylem embolism formation*

350 In the studied tropical rainforest, the leaves of most of the species would reach turgor loss point

351 before the water potential associated with the onset of xylem embolism in the leaf xylem (Fig.

352 1). This suggests that stomata close prior to the spread of leaf xylem embolism, expanding

353 recent findings showing that embolism in leaf xylem does not occur with open stomata

354 (Cardoso, Brodribb, Lucani, DaMatta, & McAdam, 2018; Creek et al., 2020; Dayer et al., 2020;

355 Hochberg et al., 2017; Li et al., 2019; Manzi et al., 2022; Skelton et al., 2018, 2021; Sorek et

356 al., 2021) to tall tropical rainforest tree species, akin to what has been shown for branches in

357 different biomes (Creek et al., 2018; Li et al., 2018; Martin-StPaul et al., 2017; Mencuccini et

358 al., 2015; Tyree & Sperry, 1988; Ziegler et al., 2019). Consequently, it is unlikely that the onset

359 of leaf xylem embolism is a signal for stomatal closure, contrary to what has been suggested by

360 several meta-analyses (e.g. Bartlett et al., 2016; Scoffoni, Sack, & Ort, 2017). A protective

361 mechanism such as early stomatal closure may be particularly important for species with narrow

362 leaf stomatal safety margins and extremely steep leaf xylem vulnerability curves (e.g. *E.*

363 *sagotiana*, *C. schomburgkianus*, *S. sp1*, *V. michelii*), in which embolism would propagate at

364 high rate. For rainforest tree species, the uncoupling of P_{tlp} and $P_{12,leaf}$ implies that a conservative

365 stomatal strategy allowing positive leaf hydraulic safety margins through timely stomatal

366 closure has been favored (Martin-StPaul et al., 2017; Creek et al., 2020), instead of

367 overoptimizing stomatal behavior with regard to leaf hydraulic risk which would maximize

368 carbon gain during mild drought (as supported by Sperry et al., 2017 and Anderegg et al., 2018).

369 This is particularly true for species that have achieved broader leaf hydraulic safety margins

370 through lower leaf xylem vulnerability to embolism, evidenced by the strong mathematical

371 dependence of P_{12} SSM_{leaf} on $P_{12,leaf}$.

372   During the normal-intensity dry season of 2018, most of the species in our study had a

373 leaf water potential at midday less negative than the leaf water potential associated with the

374 onset of leaf xylem embolism (Fig. 1; Fig. 2). These positive and sometimes large P_{12} HSM_{leaf}

375 values suggest that most species' leaves are well-protected against xylem embolism formation

376 during 'routine' seasonal droughts in this tropical rainforest. Since P_{md} was less negative than

377 P_{tlp}, we can suppose that, during a normal-intensity dry season, the trees rely on strategies

12

378 enabling them to maintain leaf gas exchange (Stahl, Burban et al., 2013), for example as

379 accessing deep soil water (Brum et al., 2018; Stahl, Hérault, et al., 2013). However, if leaf water

380 potentials would further drop during a more severe dry-season, stomatal closure may be a

381 crucial physiological mechanism to avoid xylem embolism. Indeed, leaf water potentials

382 decrease much slower when they approach P_{tlp} thanks to stomatal regulation (Hochberg et al.,

383 2017), which constrains the variation in the experienced leaf water potential. This may partly

384 explain why P_{md} varied much less than leaf xylem vulnerability to embolism. Moreover, at our

385 site, species that reach P_{tlp} earlier also exhibit less negative P_{md} values (Ziegler et al., 2019).

386 Therefore, the highly constrained values of P_{tlp} (> -3 MPa) across the rainforest tree species we

387 studied indicates that turgor loss not only precedes but may also prevent leaf xylem embolism.

388

389 4.2 *Contrasting vulnerability to drought in locally coexisting tropical rainforest tree species*

390 To our knowledge, our study provides the only empirical solving of an extensive sequence of

391 leaf and stem water potentials thresholds during dehydration for rainforest canopy tree species,

392 with the added advantage that all hydraulic traits were measured on the same individual trees.

393 The studied species differed markedly in leaf hydraulic safety margins. Notably, a few species

394 (Table 1; Fig. 1; Fig. 2) had narrow P_{12} HSM_{leaf} and significant levels of leaf xylem embolism

395 during the 2018 dry season. This result should however be considered with caution given the

396 rather small sample size for each species and high standard errors around the mean estimated

397 PLC. Given the time- and labor-intensive nature of these measurements, we also did not account

398 for within-crown variation, which may better explain leaf vulnerability patterns (Cardoso, Batz,

399 & McAdam, 2020). The sometimes rather large differences we evidenced between trees

400 belonging to the same species nevertheless suggest that the most vulnerable individuals may be

401 susceptible to dry-season embolism-induced leaf damage and/or loss under more frequent and

402 repeated severe droughts. A loss in functional leaf area due to leaf xylem embolism would

403 seriously reduce total carbon assimilation, potentially triggering a situation of carbon starvation

404 (McDowell et al., 2011, 2022) and affecting the trees' ability to recover possible losses in stem

405 hydraulic conductivity (Trugman et al., 2018). It has recently been observed that beech trees

406 suffering from drought-induced defoliation showed a limited recovery of stem xylem hydraulic

407 conductivity, accompanied with significant crown defoliation and starch depletion in the

408 following growing season (Arend et al., 2022). This effect may be more pronounced for non-

409 segmented species for which leaf loss and stem xylem embolism are closely linked (Walthert

410 et al., 2021); future extreme events may also endanger some non-segmented rainforest tree

13

species. By contrast, some species experienced strong vulnerability segmentation which would be enhanced by a more vulnerable leaf xylem and narrower leaf hydraulic safety margins, promoting drought-survival (Blackman, Li, et al., 2019).

Some of the species in our sampling are known to occasionally express deciduousness around the peak of the dry season (i.e. *D. guianensis, P. Cochlearia*; Loubry, 1994), but this phenomenon remains anecdotal at our site (Levionnois et al., 2020). Tropical rainforest evergreen species commonly exhibit a rather long leaf life span, such that the leaves may experience more than one dry seasons (Hegarty, 1990; Coste et al., 2011). The considerable leaf construction costs associated with such a long leaf life span seem to be largely offset, even during severe dry seasons, by being co-selected with low leaf xylem vulnerability to embolism, thus avoiding expensive carbon losses (Oliveira et al., 2021). This is in agreement with the absence of any observed increase in litterfall during seasonal dry periods in French Guiana, regardless of drought intensity (Wagner, Rossi, Stahl, Bonal, & Hérault, 2013). Under more severe conditions, the strong interspecific variation in leaf hydraulic safety margins and more generally in leaf and stem hydraulic traits in the studied trees (Fig. 3) may lead to marked differences in drought-induced vascular damage. Some species may therefore be subject to contrasting environmental filtering, which may alter tree community composition and species distribution (Kraft et al., 2015; Ruffault, Pimont, Cochard, Dupuy, & Martin-StPaul, 2022). In fact, it has already been shown that cross-species differences in leaf stomatal safety margins were related to tree mortality for tropical dry-forest tree species during a strong-intensity drought (Powers et al., 2020). Whether this also applies to less seasonal rainforests is a valid question. Plants may use a plethora of hydraulic strategies including limiting water losses through low residual water conductance (Duursma et al., 2019; Wolfe, 2020), vulnerability segmentation (Levionnois et al., 2020) and maintaining access to soil water through an effective deep rooting system (Brum et al., 2018; Stahl, Hérault, et al., 2013). Plus, the influence of biotic factors such as competition may be a confounding factor in investigations of the drivers of tree mortality (Pillet et al., 2018).

The strong interspecific variation in hydraulic traits we evidenced may be rooted in the long-term shaping of tree communities due to the interplay of climatic variations and species-specific demographics in the Guiana Shield (Esquivel-Muelbert, Baker, et al., 2017; Esquivel-Muelbert, Galbraith, et al., 2017). Indeed, the uncoupling of P_{tlp} and $P_{50,leaf}$ may be the result of contrasting evolutionary pressures, rather than of a deeper evolutionary integration arising from functional, developmental or genetic constraints (Sanchez-Martinez, Martinez-Vilalta, Dexter,

444   Segovia, & Mencuccini, 2020). This may be analogous to what has been suggested for stems

445   (Martin-StPaul et al., 2017; Ziegler et al., 2019).

446

447   4.3 *Comparable leaf stomatal safety margins across biomes*

448   Our literature survey suggests that some Neotropical rainforest tree species do not necessarily

449   have narrower leaf stomatal safety margins in comparison to species from other, especially

450   drier, biomes (Fig. 4). This further contradicts the idea that most rainforest tree species employ

451   a risky hydraulic strategy and underlies the broad interspecific variations in hydraulic and

452   stomatal safety margins found across biomes (Choat et al., 2012; Martin-StPaul et al., 2017; but

453   see Ziegler et al., 2019). The absence of cross-biome variation in P_{50} SSM_{leaf} we found can be

454   imputed to the broad within-biome variations in this trait, which could be driven by local water

455   availability gradients linked, for instance, to topography and/or habitat (Trueba et al., 2017;

456   Brum et al., 2018; Schmitt et al., 2020, 2021). Contrasting hydraulic strategies across species

457   may also contribute to the observed variations in P_{50} SSM_{leaf} (Pivovaroff et al., 2016; Brum et

458   al., 2018). Moreover, despite the large interspecific variation we revealed, a vast majority of

459   species showed positive and sometimes even large P_{50} SSM_{leaf} values, with the exception of

460   only three tropical dry-forest species. This highlights that early stomatal closure relative to the

461   formation of leaf xylem embolism is a common mechanism favoring delayed hydraulic

462   dysfunction across woody species. Although avoiding stem xylem embolism appears central to

463   a tree's drought survival (Brodribb & Cochard, 2010; Urli et al., 2013), our results indicate that

464   leaf xylem embolism should also be acknowledged as a non-routine event. During exceptional

465   drought, leaf xylem embolism may lead to increased tree mortality, as it has recently been

466   observed *in natura* (Powers et al., 2020). At our site, coexisting tree species exhibited broad

467   variation in leaf and stem stomatal safety margins (this study; Ziegler et al., 2019), vulnerability

468   segmentation (Levionnois et al., 2020) and residual leaf and bark conductance (Levionnois et

469   al., 2021). The coordination among these traits may influence the likelihood of tree hydraulic

470   damage and mortality risk with the increased occurrence of extreme drought events (Brodribb,

471   Powers, Cochard, & Choat, 2020). Future work should thus focus on identifying whether

472   particular traits are important in determining species vulnerability to future climatic conditions

473   in this biome.

474   The data we gathered in the tropical rainforest biome covers relatively abundant tree

475   species with contrasting habitat preferences (Allié et al., 2015; Baraloto et al., 2021). Our

476   dataset therefore represents, to a certain extent, the interspecific variation in hydraulic traits

found at our site. To have a more comprehensive understanding of the potential influence of species hydraulic traits on tree performance across lowland tropical rainforests, it would be valuable to conduct similar studies in different ecoregions with contrasting drought-intensities, for example, at the dry-edge of species' distribution range (Reis et al., 2022), including tropical rainforests in Africa and Asia for which no data is currently available. Nonetheless, the data gathered in this study could still be useful to parameterize individual-, stand- or regional-scale mechanistic models predicting rainforest tree species' survival probability during drought (Cochard, Pimont, Ruffault, & Martin-StPaul, 2021; Ruffault et al., 2022). Our data may also serve to improve predictions of carbon fluxes at the regional scale, by incorporating them into hydraulic models embedded in process-based land surface models (Eller et al., 2020; Fisher & Koven, 2020; Papastefanou et al., 2020; Li et al. 2021).

5 CONCLUSIONS

We evidenced that most of the species in this study do not reach turgor loss point and could potentially still maintain leaf gas exchange during a normal-intensity dry season. Yet, under hypothetically more severe droughts, turgor loss and thus probable subsequent stomatal closure are likely to strongly limit plant water loss. This mechanism may delay the onset of xylem embolism in rainforest canopy tree species. In line with these findings, we also corroborate the hypothesis that, regardless of the considered biome, leaf xylem embolism is not a triggering signal for leaf-cell turgor loss. The uncoupling of these two mechanisms may allow the avoidance of hydraulic dysfunction as a result of selective pressures favoring tree drought survival under drier conditions, with species with the lowest leaf vulnerability to xylem embolism achieving higher leaf hydraulic and stomatal safety margins. As such, this study extends the pattern found by Creek et al., (2020) to tropical rainforest tree species. Whether or not tropical rainforest tree species of the Guyana Shield will be subject to drought-induced defoliation or increased mortality in the near future is a crucial question. The present study brings novel insight to this matter by proving the ability of most tropical rainforest tree species to nearly systematically avoid the formation of xylem embolism during the dry season. However, some species may be more vulnerable than others. By comparing leaf stomatal safety margins across biomes, we corroborate that tropical rainforest species may employ a conservative stomatal strategy with regard to hydraulic risk, akin to species from drier biomes. Finally, our data provide an opportunity to parameterize trait-based models with greater realism

509 to better predict the fate of tropical rainforests, and the already ongoing broad-scale shifts in
510 their floristic and functional tree community composition (Esquivel-Muelbert et al., 2019).

511

529

530 **CONFLICT OF INTEREST**
531 The authors declare having no conflicts of interest.

532

533 **DATA AVAILABILITY STATEMENT**
534 All data corresponding to species' mean trait values are included in the manuscript. All raw
535 data generated during current can be found in the supplementary material (Table S2). The data
536 gathered for the literature survey will be made accessible via the Dryad Digital Repository.

537

538 **AUTHOR'S CONTRIBUTIONS**
539 CZ and SL conceived the ideas of the study; CZ, SL, CS, PH, DB and SC designed the original
540 experiments, collected field samples, performed measurements, or provided data; CZ and SL
541 performed data analysis; CZ and SL led the writing of the manuscript; all authors contributed

17

542   critically to the draft and approved the submitted version.

543

544 **REFERENCES**

545 Aguilos, M., Stahl, C., Burban, B., Hérault, B., Courtois, E., Coste, S., . . . Bonal, D. (2019).
546   Interannual and seasonal variations in ecosystem transpiration and water use efficiency
547   in a tropical rainforest. *Forests, 10*(1), 14. doi:10.3390/f10010014

548 Allie, E., Pelissier, R., Engel, J., Petronelli, P., Freycon, V., Deblauwe, V., . . . Baraloto, C.
549   (2015). Pervasive Local-Scale Tree-Soil Habitat Association in a Tropical Forest
550   Community. *PLoS One, 10*(11), e0141488. doi:10.1371/journal.pone.0141488

551 Anderegg, W. R., Klein, T., Bartlett, M., Sack, L., Pellegrini, A. F., Choat, B., & Jansen, S.
552   (2016). Meta-analysis reveals that hydraulic traits explain cross-species patterns of
553   drought-induced tree mortality across the globe. *Proc Natl Acad Sci U S A, 113*(18),
554   5024-5029. doi:10.1073/pnas.1525678113

555 Anderegg, W. R. L., Wolf, A., Arango-Velez, A., Choat, B., Chmura, D. J., Jansen, S., . . .
556   Pacala, S. (2018). Woody plants optimise stomatal behaviour relative to hydraulic risk.
557   *Ecol Lett, 21*(7), 968-977. doi:10.1111/ele.12962

558 Arend, M., Link, R. M., Zahnd, C., Hoch, G., Schuldt, B., & Kahmen, A. (2022). Lack of
559   hydraulic recovery as cause of post-drought foliage reduction and canopy decline in
560   European beech. *New Phytologist*. *234*(4), 1195-1205. doi: 10.1111/nph.18065

561 Baraloto, C., Vleminckx, J., Engel, J., Petronelli, P., Dávila, N., RÍos, M., . . . Fortunel, C.
562   (2021). Biogeographic history and habitat specialization shape floristic and
563   phylogenetic composition across Amazonian forests. *Ecological Monographs, 91*(4),
564   e01473. doi: 10.1002/ecm.1473

565 Barros, F. V., Bittencourt, P. R. L., Brum, M., Restrepo-Coupe, N., Pereira, L., Teodoro, G. S.,
566   . . . Oliveira, R. S. (2019). Hydraulic traits explain differential responses of Amazonian
567   forests to the 2015 El Nino-induced drought. *New Phytol, 223*(3), 1253-1266.
568   doi:10.1111/nph.15909

569 Bartlett, M. K., Klein, T., Jansen, S., Choat, B., & Sack, L. (2016). The correlations and
570   sequence of plant stomatal, hydraulic, and wilting responses to drought. *Proc Natl Acad
571   Sci U S A, 113*(46), 13098-13103. doi:10.1073/pnas.1604088113

572 Blackman, C. J., Creek, D., Maier, C., Aspinwall, M. J., Drake, J. E., Pfautsch, S., . . . Choat,
573   B. (2019). Drought response strategies and hydraulic traits contribute to mechanistic
574   understanding of plant dry-down to hydraulic failure. *Tree Physiol, 39*(6), 910-924.
575   doi:10.1093/treephys/tpz016

576   Blackman, C. J., Li, X., Choat, B., Rymer, P. D., De Kauwe, M. G., Duursma, R. A., . . .
577   Medlyn, B. E. (2019). Desiccation time during drought is highly predictable across
578   species of Eucalyptus from contrasting climates. *New Phytol, 224*(2), 632-643.
579   doi:10.1111/nph.16042

580   Bonal, D., Barigah, T. S., Granier, A., & Guehl, J. M. (2001). Late-stage canopy tree species
581   with extremely low δ13C and high stomatal sensitivity to seasonal soil drought in the
582   tropical rainforest of French Guiana. *Plant Cell Environ, 23*(5), 445-459.
583   doi:10.1046/j.1365-3040.2000.00556.x

584   Brodribb, Brodersen, C. R., Carriqui, M., Tonet, V., Rodriguez Dominguez, C., & McAdam,
585   S. (2021). Linking xylem network failure with leaf tissue death. *New Phytol, 232*(1),
586   68-79. doi:10.1111/nph.17577

587   Brodribb, T. J., Bienaime, D., & Marmottant, P. (2016). Revealing catastrophic failure of leaf
588   networks under stress. *Proc Natl Acad Sci U S A, 113*(17), 4865-4869.
589   doi:10.1073/pnas.1522569113

590   Brodribb, T. J., Bowman, D. J., Nichols, S., Delzon, S., & Burlett, R. (2010). Xylem function
591   and growth rate interact to determine recovery rates after exposure to extreme water
592   deficit. *New Phytol, 188*(2), 533-542. doi:10.1111/j.1469-8137.2010.03393.x

593   Brodribb, T. J., & Holbrook, N. M. (2003). Stomatal closure during leaf dehydration,
594   correlation with other leaf physiological traits. *Plant Physiol, 132*(4), 2166-2173.
595   doi:10.1104/pp.103.023879

596   Brodribb, T. J., Holbrook, N. M., Edwards, E. J., & GutiÉRrez, M. V. (2003). Relations
597   between stomatal closure, leaf turgor and xylem vulnerability in eight tropical dry forest
598   trees. *Plant Cell Environ, 26*(3), 443-450. doi:10.1046/j.1365-3040.2003.00975.x

599   Brodribb, T. J., Powers, J., Cochard, H., & Choat, B. (2020). Hanging by a thread? Forests and
600   drought. *Science, 368*(6488), 261-266. doi:10.1126/science.aat7631

601   Brodribb, T. J., Skelton, R. P., McAdam, S. A., Bienaime, D., Lucani, C. J., & Marmottant, P.
602   (2016). Visual quantification of embolism reveals leaf vulnerability to hydraulic failure.
603   *New Phytol, 209*(4), 1403-1409. doi:10.1111/nph.13846

604   Brum, M., Vadeboncoeur, M. A., Ivanov, V., Asbjornsen, H., Saleska, S., Alves, L. F., . . .
605   Barua, D. (2018). Hydrological niche segregation defines forest structure and drought
606   tolerance strategies in a seasonal Amazon forest. *Journal of Ecology, 107*(1), 318-333.
607   doi:10.1111/1365-2745.13022

608 Buckley, T. N. (2019). How do stomata respond to water status? *New Phytol, 224*(1), 21-36.
609   doi:10.1111/nph.15899

610 Burlett, R., Parise, C., Capdeville, G., Cochard, H., Lamarque, L. J., King, A., & Delzon, S.
611   (2022). Measuring xylem hydraulic vulnerability for long-vessel species: an improved
612   methodology with the flow centrifugation technique. *Annals of Forest Science, 79*(1),
613   1-16. doi:10.1186/s13595-022-01124-0

614 Cardoso, A. A., Brodribb, T. J., Lucani, C. J., DaMatta, F. M., & McAdam, S. A. M. (2018).
615   Coordinated plasticity maintains hydraulic safety in sunflower leaves. *Plant Cell
616   Environ, 41*(11), 2567-2576. doi:10.1111/pce.13335

617 Cardoso, A. A., Batz, T. A., & McAdam, S. A. (2020). Xylem embolism resistance determines
618   leaf mortality during drought in Persea americana. *Plant Physiol, 182*(1), 547-554. doi:
619   10.1104/pp.19.00585

620 Choat, B., Brodribb, T. J., Brodersen, C. R., Duursma, R. A., Lopez, R., & Medlyn, B. E.
621   (2018). Triggers of tree mortality under drought. *Nature, 558*(7711), 531-539.
622   doi:10.1038/s41586-018-0240-x

623 Choat, B., Jansen, S., Brodribb, T. J., Cochard, H., Delzon, S., Bhaskar, R., . . . Zanne, A. E.
624   (2012). Global convergence in the vulnerability of forests to drought. *Nature,
625   491*(7426), 752-755. doi:10.1038/nature11688

626 Cochard, H. (2006). Cavitation in trees. *Comptes Rendus Physique, 7*(9-10), 1018-1026.
627   doi:10.1016/j.crhy.2006.10.012

628 Cochard, H., Pimont, F., Ruffault, J., & Martin-StPaul, N. (2021). SurEau: a mechanistic model
629   of plant water relations under extreme drought. *Annals of Forest Science, 78*(2), 1-23.
630   doi: 10.1007/s13595-021-01067-y

631 Coste, S., Roggy, J. C., Schimann, H., Epron, D., & Dreyer, E. (2011). A cost-benefit analysis
632   of acclimation to low irradiance in tropical rainforest tree seedlings: leaf life span and
633   payback time for leaf deployment. *J Exp Bot, 62*(11), 3941-3955.
634   doi:10.1093/jxb/err092

635 Creek, D., Blackman, C. J., Brodribb, T. J., Choat, B., & Tissue, D. T. (2018). Coordination
636   between leaf, stem, and root hydraulics and gas exchange in three arid-zone
637   angiosperms during severe drought and recovery. *Plant Cell Environ, 41*(12), 2869-
638   2881. doi:10.1111/pce.13418

639 Creek, D., Lamarque, L. J., Torres-Ruiz, J. M., Parise, C., Burlett, R., Tissue, D. T., & Delzon,
640   S. (2020). Xylem embolism in leaves does not occur with open stomata: evidence from

direct observations using the optical visualization technique. *J Exp Bot, 71*(3), 1151-1159. doi:10.1093/jxb/erz474

Dayer, S., Herrera, J. C., Dai, Z., Burlett, R., Lamarque, L. J., Delzon, S., . . . Gambetta, G. A. (2020). The sequence and thresholds of leaf hydraulic traits underlying grapevine varietal differences in drought tolerance. *J Exp Bot, 71*(14), 4333-4344. doi:10.1093/jxb/eraa186

Duursma, R. A., Blackman, C. J., Lopez, R., Martin-StPaul, N. K., Cochard, H., & Medlyn, B. E. (2019). On the minimum leaf conductance: its role in models of plant water use, and ecological and environmental controls. *New Phytol, 221*(2), 693-705. doi:10.1111/nph.15395

Duursma, R. A., & Choat, B. (2017). fitplc: an R package to fit hydraulic vulnerability curves. *Journal of Plant Hydraulics*. doi: 10.20870/jph.2017.e002

Eller, C. B., Rowland, L., Mencuccini, M., Rosas, T., Williams, K., Harper, A., . . . Cox, P. M. (2020). Stomatal optimization based on xylem hydraulics (SOX) improves land surface model simulation of vegetation responses to climate. *New Phytol, 226*(6), 1622-1637. doi:10.1111/nph.16419

Esquivel-Muelbert, A., Baker, T. R., Dexter, K. G., Lewis, S. L., Brienen, R. J. W., Feldpausch, T. R., . . . Phillips, O. L. (2019). Compositional response of Amazon forests to climate change. *Glob Chang Biol, 25*(1), 39-56. doi:10.1111/gcb.14413

Esquivel-Muelbert, A., Baker, T. R., Dexter, K. G., Lewis, S. L., ter Steege, H., Lopez-Gonzalez, G., . . . Phillips, O. L. (2017). Seasonal drought limits tree species across the Neotropics. *Ecography, 40*(5), 618-629. doi:10.1111/ecog.01904

Esquivel-Muelbert, A., Galbraith, D., Dexter, K. G., Baker, T. R., Lewis, S. L., Meir, P., . . . Phillips, O. L. (2017). Biogeographic distributions of neotropical trees reflect their directly measured drought tolerances. *Sci Rep, 7*(1), 8334. doi:10.1038/s41598-017-08105-8

Fisher, R. A., & Koven, C. D. (2020). Perspectives on the future of land surface models and the challenges of representing complex terrestrial systems. *Journal of Advances in Modeling Earth Systems, 12*(4), e2018MS001453. doi: 10.1029/2018MS001453

Fontes, C. G., Fine, P. V., Wittmann, F., Bittencourt, P. R., Piedade, M. T. F., Higuchi, N., . . . Dawson, T. E. (2020). Convergent evolution of tree hydraulic traits in Amazonian habitats: implications for community assemblage and vulnerability to drought. *New Phytologist, 228*(1), 106-120. doi: 10.1111/nph.16675

Gauthey, A., Peters, J. M. R., Lopez, R., Carins-Murphy, M. R., Rodriguez-Dominguez, C. M., Tissue, D. T., . . . Choat, B. (2022). Mechanisms of xylem hydraulic recovery after drought in Eucalyptus saligna. *Plant Cell Environ, 45*(4), 1216-1228. doi:10.1111/pce.14265

678   Gourlet-Fleury, S., Guehl, J. M., & Laroussinie, O. (2004). *Ecology and Management of a*
679   *Neotropical Rainforest. Lessons drawn from Paracou, a long-term experimental*
680   *research site in French Guiana.* Paris: Elsevier.

681   Hartmann, H., Bastos, A., Das, A. J., Esquivel-Muelbert, A., Hammond, W. M., Martínez-
682   Vilalta, J., . . . Ruthrof, K. X. (2022). Climate Change Risks to Global Forest Health:
683   Emergence of Unexpected Events of Elevated Tree Mortality Worldwide. *Annual*
684   *review of plant biology, 73*. doi: 10.1146/annurev-arplant-102820-012804

685   Hegarty, E. E. (1990). Leaf life-span and leafing phenology of lianes and associated trees during
686   a rainforest succession. *The Journal of Ecology*, 300-312.

687   Hochberg, U., Albuquerque, C., Rachmilevitch, S., Cochard, H., David-Schwartz, R.,
688   Brodersen, C. R., . . . Windt, C. W. (2016). Grapevine petioles are more sensitive to
689   drought induced embolism than stems: evidence from in vivo MRI and microcomputed
690   tomography observations of hydraulic vulnerability segmentation. *Plant Cell Environ,*
691   *39*(9), 1886-1894. doi:10.1111/pce.12688

692   Hochberg, U., Rockwell, F. E., Holbrook, N. M., & Cochard, H. (2018). Iso/Anisohydry: A
693   Plant-Environment Interaction Rather Than a Simple Hydraulic Trait. *Trends Plant Sci,*
694   *23*(2), 112-120. doi:10.1016/j.tplants.2017.11.002

695   Hochberg, U., Windt, C. W., Ponomarenko, A., Zhang, Y. J., Gersony, J., Rockwell, F. E., &
696   Holbrook, N. M. (2017). Stomatal Closure, Basal Leaf Embolism, and Shedding Protect
697   the Hydraulic Integrity of Grape Stems. *Plant Physiol, 174*(2), 764-775.
698   doi:10.1104/pp.16.01816

699   Huntingford, C., Zelazowski, P., Galbraith, D., Mercado, L. M., Sitch, S., Fisher, R., . . . Booth,
700   B. B. (2013). Simulated resilience of tropical rainforests to CO2-induced climate
701   change. *Nature Geoscience, 6*(4), 268-273. doi:ngeo1741

702   Jacobsen, A. L., Pratt, R. B., Tobin, M. F., Hacke, U. G., & Ewers, F. W. (2012). A global
703   analysis of xylem vessel length in woody plants. *American Journal of Botany, 99*(10),
704   1583-1591. doi:10.3732/ajb.1200140

705   Johnson, D. M., Woodruff, D. R., McCulloh, K. A., & Meinzer, F. C. (2009). Leaf hydraulic
706   conductance, measured in situ, declines and recovers daily: leaf hydraulics, water
707   potential and stomatal conductance in four temperate and three tropical tree species.
708   *Tree Physiol, 29*(7), 879-887. doi:10.1093/treephys/tpp031

709 Johnson, K. M., Jordan, G. J., & Brodribb, T. J. (2018). Wheat leaves embolized by water stress
710   do not recover function upon rewatering. *Plant Cell Environ, 41*(11), 2704-2714.
711   doi:10.1111/pce.13397

712 Klepsch, M., Zhang, Y., Kotowska, M. M., Lamarque, L. J., Nolf, M., Schuldt, B., . . . Jansen,
713   S. (2018). Is xylem of angiosperm leaves less resistant to embolism than branches?
714   Insights from microCT, hydraulics, and anatomy. *J Exp Bot, 69*(22), 5611-5623.
715   doi:10.1093/jxb/ery321

716 Kraft, N. J., Adler, P. B., Godoy, O., James, E. C., Fuller, S., & Levine, J. M. (2015).
717   Community assembly, coexistence and the environmental filtering metaphor.
718   *Functional Ecology, 29*(5), 592-599. doi:10.1111/1365-2435.12345

719 Levionnois, S., Ziegler, C., Heuret, P., Jansen, S., Stahl, C., Calvet, E., . . . Coste, S. (2021). Is
720   vulnerability segmentation at the leaf-stem transition a drought resistance mechanism?
721   A theoretical test with a trait-based model for Neotropical canopy tree species. *Annals*
722   *of Forest Science, 78*(4), 1-16. doi:10.1007/s13595-021-01094-9

723 Levionnois, S., Ziegler, C., Jansen, S., Calvet, E., Coste, S., Stahl, C., . . . Heuret, P. (2020).
724   Vulnerability and hydraulic segmentations at the stem-leaf transition: coordination
725   across Neotropical trees. *New Phytol, 228*(2), 512-524. doi:10.1111/nph.16723

726 Li, L., Yang, Z. L., Matheny, A. M., Zheng, H., Swenson, S. C., Lawrence, D. M., . . . Leung,
727   L. R. (2021). Representation of plant hydraulics in the Noah-MP land surface model:
728   Model development and multiscale evaluation. *Journal of Advances in Modeling Earth*
729   *Systems, 13*(4), e2020MS002214. doi:10.1029/2020MS002214

730 Li, X., Blackman, C. J., Choat, B., Duursma, R. A., Rymer, P. D., Medlyn, B. E., & Tissue, D.
731   T. (2018). Tree hydraulic traits are coordinated and strongly linked to climate-of-origin
732   across a rainfall gradient. *Plant Cell Environ, 41*(3), 646-660. doi:10.1111/pce.13129

733 Li, X., Blackman, C. J., Peters, J. M. R., Choat, B., Rymer, P. D., Medlyn, B. E., . . . Oliveira,
734   R. (2019). More than iso/anisohydry: Hydroscapes integrate plant water use and drought
735   tolerance traits in 10 eucalypt species from contrasting climates. *Functional Ecology,*
736   *33*(6), 1035-1049. doi:10.1111/1365-2435.13320

737 Li, X., Delzon, S., Torres-Ruiz, J., Badel, E., Burlett, R., Cochard, H., . . . Choat, B. (2020).
738   Lack of vulnerability segmentation in four angiosperm tree species: evidence from
739   direct X-ray microtomography observation. *Annals of Forest Science, 77*(2).
740   doi:10.1007/s13595-020-00944-2

741   Lo Gullo, M. A., Nardini, A., Trifilò, P., & Salleo, S. (2003). Changes in leaf hydraulics and
742   stomatal conductance following drought stress and irrigation in Ceratonia siliqua (Carob
743   tree). *Physiologia Plantarum, 117*(2), 186-194. doi:10.1034/j.1399-3054.2003.00038.x

744   Loubry, D. (1994). La phénologie des arbres caducifoliés en forêt guyanaise (5° de latitude
745   nord): illustration d'un déterminisme à composantes endogène et exogène. *Canadian
746   Journal of Botany, 72*(12), 1843-1857. doi:10.1139/b94-226

747   Manzi, O. J. L., Bellifa, M., Ziegler, C., Mihle, L., Levionnois, S., Burban, B., . . . Stahl, C.
748   (2022). Drought stress recovery of hydraulic and photochemical processes in
749   Neotropical tree saplings. *Tree Physiol, 42*(1), 114-129. doi:10.1093/treephys/tpab092

750   Maréchaux, I., Bonal, D., Bartlett, M. K., Burban, B., Coste, S., Courtois, E. A., . . . Sala, A.
751   (2018). Dry-season decline in tree sapflux is correlated with leaf turgor loss point in a
752   tropical rainforest. *Functional Ecology, 32*(10), 2285-2297. doi:10.1111/1365-
753   2435.13188

754   Martin-StPaul, N., Delzon, S., & Cochard, H. (2017). Plant resistance to drought depends on
755   timely stomatal closure. *Ecol Lett, 20*(11), 1437-1447. doi:10.1111/ele.12851

756   McDowell, N. G., Beerling, D. J., Breshears, D. D., Fisher, R. A., Raffa, K. F., & Stitt, M.
757   (2011). The interdependence of mechanisms underlying climate-driven vegetation
758   mortality. *Trends Ecol Evol, 26*(10), 523-532. doi:10.1016/j.tree.2011.06.003

759   McDowell, N. G., Sapes, G., Pivovaroff, A., Adams, H. D., Allen, C. D., Anderegg, W. R., . . .
760   Choat, B. (2022). Mechanisms of woody-plant mortality under rising drought, CO2 and
761   vapour pressure deficit. *Nature Reviews Earth & Environment*, 1-15. doi:s43017-022-
762   00272-1

763   Meinzer, F. C., Johnson, D. M., Lachenbruch, B., McCulloh, K. A., & Woodruff, D. R. (2009).
764   Xylem hydraulic safety margins in woody plants: coordination of stomatal control of
765   xylem tension with hydraulic capacitance. *Functional Ecology, 23*(5), 922-930.
766   doi:10.1111/j.1365-2435.2009.01577.x

767   Mencuccini, M., Minunno, F., Salmon, Y., Martinez-Vilalta, J., & Holtta, T. (2015).
768   Coordination of physiological traits involved in drought-induced mortality of woody
769   plants. *New Phytol, 208*(2), 396-409. doi:10.1111/nph.13461

770   Nardini, A., & Salleo, S. (2000). Limitation of stomatal conductance by hydraulic traits: sensing
771   or preventing xylem cavitation? *Trees, 15*(1), 14-24. doi:10.1007/s004680000071

772 Nardini, A., Tyree, M. T., & Salleo, S. (2001). Xylem cavitation in the leaf of Prunus
773   laurocerasus and its impact on leaf hydraulics. *Plant Physiol, 125*(4), 1700-1709.
774   doi:10.1104/pp.125.4.1700

775 Ocheltree, T., Gleason, S., Cao, K.-F., & Jiang, G.-F. (2020). Loss and recovery of leaf
776   hydraulic conductance: Root pressure, embolism, and extra-xylary resistance. *Journal*
777   *of Plant Hydraulics, 7*. doi:10.20870/jph.2020.e-001

778 Oliveira, R. S., Eller, C. B., Barros, F. d. V., Hirota, M., Brum, M., & Bittencourt, P. (2021).
779   Linking plant hydraulics and the fast–slow continuum to understand resilience to
780   drought in tropical ecosystems. *New Phytologist, 230*(3), 904-923.
781   doi:10.1111/nph.17266

782 Pammenter, N. W., & Van der Willigen, C. (1998). A mathematical and statistical analysis of
783   the curves illustrating vulnerability of xylem to cavitation. *Tree Physiology, 18*(8-9),
784   589-593. doi:10.1093/treephys/18.8-9.589

785 Papastefanou, P., Zang, C. S., Pugh, T. A., Liu, D., Grams, T. E., Hickler, T., & Rammig, A.
786   (2020). A dynamic model for strategies and dynamics of plant water-potential
787   regulation under drought conditions. *Frontiers in Plant Science*, 373.
788   doi:10.3389/fpls.2020.00373

789 Pillet, M., Joetzjer, E., Belmin, C., Chave, J., Ciais, P., Dourdain, A., . . . Zhou, S. (2018).
790   Disentangling competitive vs. climatic drivers of tropical forest mortality. *Journal of*
791   *Ecology, 106*(3), 1165-1179. doi:10.1111/1365-2745.12876

792 Pivovaroff, A. L., Pasquini, S. C., De Guzman, M. E., Alstad, K. P., Stemke, J. S., Santiago, L.
793   S., & Field, K. (2016). Multiple strategies for drought survival among woody plant
794   species. *Functional Ecology, 30*(4), 517-526. doi:10.1111/1365-2435.12518

795 Powers, J. S., Vargas, G. G., Brodribb, T. J., Schwartz, N. B., Perez-Aviles, D., Smith-Martin,
796   C. M., . . . Medvigy, D. (2020). A catastrophic tropical drought kills hydraulically
797   vulnerable tree species. *Glob Chang Biol, 26*(5), 3122-3133. doi:10.1111/gcb.15037

798 R Core Team (2018) R: A language and environment for statistical computing. R Foundation
799   for Statistical Computing, Vienna, Austria. https://www.R-project.org/ (May, 2022)

800 Reis, S. M., Marimon, B. S., Esquivel-Muelbert, A., Marimon Jr, B. H., Morandi, P. S., Elias,
801   F., . . . Menor, I. O. (2022). Climate and crown damage drive tree mortality in southern
802   Amazonian edge forests. *Journal of Ecology, 110*(4), 876-888. doi:10.1111/1365-
803   2745.13849

804 Rodriguez-Dominguez, C. M., Buckley, T. N., Egea, G., de Cires, A., Hernandez-Santana, V.,
805   Martorell, S., & Diaz-Espejo, A. (2016). Most stomatal closure in woody species under
806   moderate drought can be explained by stomatal responses to leaf turgor. *Plant Cell*
807   *Environ, 39*(9), 2014-2026. doi:10.1111/pce.12774

808   Rodriguez-Dominguez, C. M., Carins Murphy, M. R., Lucani, C., & Brodribb, T. J. (2018).
809   Mapping xylem failure in disparate organs of whole plants reveals extreme resistance
810   in olive roots. *New Phytol, 218*(3), 1025-1035. doi:10.1111/nph.15079

811   Ruffault, J., Pimont, F., Cochard, H., Dupuy, J.-L., & Martin-StPaul, N. K. (2022). SurEau-
812   Ecos v2. 0: A trait-based plant hydraulics model for simulations of plant water status
813   and drought-induced mortality at the ecosystem level. *Geoscientific Model*
814   *Development Discussions*, 1-47. doi:10.5194/gmd-15-5593-2022

815   Sanchez-Martinez, P., Martinez-Vilalta, J., Dexter, K. G., Segovia, R. A., & Mencuccini, M.
816   (2020). Adaptation and coordinated evolution of plant hydraulic traits. *Ecol Lett, 23*(11),
817   1599-1610. doi:10.1111/ele.13584

818   Savi, T., Marin, M., Luglio, J., Petruzzellis, F., Mayr, S., & Nardini, A. (2016). Leaf hydraulic
819   vulnerability protects stem functionality under drought stress in Salvia officinalis. *Funct*
820   *Plant Biol, 43*(4), 370-379. doi:10.1071/FP15324

821   Schenk, H. J., Jansen, S., & Hölttä, T. (2020). Positive pressure in xylem and its role in
822   hydraulic function. *New Phytologist*. doi:10.1111/nph.17085

823   Schmitt, S., Hérault, B., Ducouret, É., Baranger, A., Tysklind, N., Heuertz, M., . . . Derroire,
824   G. (2020). Topography consistently drives intra-and inter-specific leaf trait variation
825   within tree species complexes in a Neotropical forest. *Oikos*. doi:10.1111/oik.07488

826   Schmitt, S., Tysklind, N., Derroire, G., Heuertz, M., & Hérault, B. (2021). Topography shapes
827   the local coexistence of tree species within species complexes of Neotropical forests.
828   *Oecologia, 196*(2), 389-398. doi:10.1007/s00442-021-04939-2

829   Scoffoni, C., Albuquerque, C., Brodersen, C. R., Townes, S. V., John, G. P., Bartlett, M. K., . .
830   . Sack, L. (2017). Outside-Xylem Vulnerability, Not Xylem Embolism, Controls Leaf
831   Hydraulic Decline during Dehydration. *Plant Physiol, 173*(2), 1197-1210.
832   doi:10.1104/pp.16.01643

833   Scoffoni, C., Albuquerque, C., Brodersen, C. R., Townes, S. V., John, G. P., Cochard, H., . . .
834   Sack, L. (2017). Leaf vein xylem conduit diameter influences susceptibility to embolism
835   and hydraulic decline. *New Phytol, 213*(3), 1076-1092. doi:10.1111/nph.14256

836   Scoffoni, C., Chatelet, D. S., Pasquet-Kok, J., Rawls, M., Donoghue, M. J., Edwards, E. J., &
837   Sack, L. (2016). Hydraulic basis for the evolution of photosynthetic productivity. *Nat*
838   *Plants, 2*(6), 16072. doi:10.1038/nplants.2016.72

839   Scoffoni, C., Sack, L., & Ort, D. (2017). The causes and consequences of leaf hydraulic decline
840   with dehydration. *J Exp Bot, 68*(16), 4479-4496. doi:10.1093/jxb/erx252

841 Skelton, R. P., Anderegg, L. D., Diaz, J., Kling, M. M., Papper, P., Lamarque, L. J., . . . Ackerly,
842   D. D. (2021). Evolutionary relationships between drought-related traits and climate
843   shape large hydraulic safety margins in western North American oaks. *Proceedings of*
844   *the National Academy of Sciences, 118*(10). doi:10.1073/pnas.2008987118

845 Skelton, R. P., Brodribb, T. J., & Choat, B. (2017). Casting light on xylem vulnerability in an
846   herbaceous species reveals a lack of segmentation. *New Phytol, 214*(2), 561-569.
847   doi:10.1111/nph.14450

848 Skelton, R. P., Dawson, T. E., Thompson, S. E., Shen, Y., Weitz, A. P., & Ackerly, D. (2018).
849   Low Vulnerability to Xylem Embolism in Leaves and Stems of North American Oaks.
850   *Plant Physiol, 177*(3), 1066-1077. doi:10.1104/pp.18.00103

851 Smith-Martin, C. M., Skelton, R. P., Johnson, K. M., Lucani, C., & Brodribb, T. J. (2020). Lack
852   of vulnerability segmentation among woody species in a diverse dry sclerophyll
853   woodland community. *Functional Ecology, 34*(4), 777-787. doi:10.1111/1365-
854   2435.13519

855 Sorek, Y., Greenstein, S., Netzer, Y., Shtein, I., Jansen, S., & Hochberg, U. (2021). An increase
856   in xylem embolism resistance of grapevine leaves during the growing season is
857   coordinated with stomatal regulation, turgor loss point and intervessel pit membranes.
858   *New Phytol, 229*(4), 1955-1969. doi:10.1111/nph.17025

859 Sperry, J. S., Hacke, U. G., Oren, R., & Comstock, J. P. (2002). Water deficits and hydraulic
860   limits to leaf water supply. *Plant Cell Environ, 25*(2), 251-263. doi:10.1046/j.0016-
861   8025.2001.00799.x

862 Sperry, J. S., Venturas, M. D., Anderegg, W. R. L., Mencuccini, M., Mackay, D. S., Wang, Y.,
863   & Love, D. M. (2017). Predicting stomatal responses to the environment from the
864   optimization of photosynthetic gain and hydraulic cost. *Plant Cell Environ, 40*(6), 816-
865   830. doi:10.1111/pce.12852

866 Stahl, C., Burban, B., Wagner, F., Goret, J.-Y., Bompy, F., & Bonal, D. (2013). Influence of
867   Seasonal Variations in Soil Water Availability on Gas Exchange of Tropical Canopy
868   Trees. *Biotropica, 45*(2), 155-164. doi:10.1111/j.1744-7429.2012.00902.x

869 Stahl, C., Herault, B., Rossi, V., Burban, B., Brechet, C., & Bonal, D. (2013). Depth of soil
870   water uptake by tropical rainforest trees during dry periods: does tree dimension matter?
871   *Oecologia, 173*(4), 1191-1201. doi:10.1007/s00442-013-2724-6

872 Torres-Ruiz, J. M., Diaz-Espejo, A., Perez-Martin, A., & Hernandez-Santana, V. (2015). Role
873   of hydraulic and chemical signals in leaves, stems and roots in the stomatal behaviour

874   of olive trees under water stress and recovery conditions. *Tree Physiol, 35*(4), 415-424.

875   doi:10.1093/treephys/tpu055

876 Trueba, S., Pan, R., Scoffoni, C., John, G. P., Davis, S. D., & Sack, L. (2019). Thresholds for

877   leaf damage due to dehydration: declines of hydraulic function, stomatal conductance

878   and cellular integrity precede those for photochemistry. *New Phytol, 223*(1), 134-149.

879   doi:10.1111/nph.15779

880 Trueba, S., Pouteau, R., Lens, F., Feild, T. S., Isnard, S., Olson, M. E., & Delzon, S. (2017).

881   Vulnerability to xylem embolism as a major correlate of the environmental distribution

882   of rain forest species on a tropical island. *Plant Cell Environ, 40*(2), 277-289.

883   doi:10.1111/pce.12859

884 Trugman, A. T., Detto, M., Bartlett, M. K., Medvigy, D., Anderegg, W. R. L., Schwalm, C., . .

885   . Pacala, S. W. (2018). Tree carbon allocation explains forest drought-kill and recovery

886   patterns. *Ecol Lett, 21*(10), 1552-1560. doi:10.1111/ele.13136

887 Tyree, M. T., & Sperry, J. S. (1988). Do woody plants operate near the point of catastrophic

888   xylem dysfunction caused by dynamic water stress? : answers from a model. *Plant*

889   *Physiol, 88*(3), 574-580. doi:10.1104/pp.88.3.574

890 Urli, M., Porte, A. J., Cochard, H., Guengant, Y., Burlett, R., & Delzon, S. (2013). Xylem

891   embolism threshold for catastrophic hydraulic failure in angiosperm trees. *Tree Physiol,*

892   *33*(7), 672-683. doi:10.1093/treephys/tpt030

893 Vargas G, G., Brodribb, T. J., Dupuy, J. M., González-M, R., Hulshof, C. M., Medvigy, D., . .

894   . Schwartz, N. B. (2021). Beyond leaf habit: generalities in plant function across 97

895   tropical dry forest tree species. *New Phytologist, 232*(1), 148-161.

896   doi:10.1111/nph.17584

897 Wagner, F., Rossi, V., Stahl, C., Bonal, D., & Hérault, B. (2013). Asynchronism in leaf and

898   wood production in tropical forests: a study combining satellite and ground-based

899   measurements. *Biogeosciences, 10*(11), 7307-7321. doi:10.5194/bg-10-7307-2013

900 Walthert, L., Ganthaler, A., Mayr, S., Saurer, M., Waldner, P., Walser, M., . . . von Arx, G.

901   (2021). From the comfort zone to crown dieback: Sequence of physiological stress

902   thresholds in mature European beech trees across progressive drought. *Science of The*

903   *Total Environment, 753*, 141792. doi:10.1016/j.scitotenv.2020.141792

904 Wolfe, B. T. (2020). Bark water vapour conductance is associated with drought performance in

905   tropical trees. *Biol Lett, 16*(8), 20200263. doi:10.1098/rsbl.2020.0263

906   Yan, C.-L., Ni, M.-Y., Cao, K.-F., & Zhu, S.-D. (2020). Leaf hydraulic safety margin and
907   safety–efficiency trade-off across angiosperm woody species. *Biology letters, 16*(11),
908   20200456. doi:10.1098/rsbl.2020.0456

909   Yao, G. Q., Nie, Z. F., Turner, N. C., Li, F. M., Gao, T. P., Fang, X. W., & Scoffoni, C. (2021).
910   Combined high leaf hydraulic safety and efficiency provides drought tolerance in
911   Caragana species adapted to low mean annual precipitation. *New Phytol, 229*(1), 230-
912   244. doi:10.1111/nph.16845

913   Zhu, S. D., Chen, Y. J., Ye, Q., He, P. C., Liu, H., Li, R. H., . . . Cao, K. F. (2018). Leaf turgor
914   loss point is correlated with drought tolerance and leaf carbon economics traits. *Tree
915   Physiol, 38*(5), 658-663. doi:10.1093/treephys/tpy013

916   Ziegler, C., Coste, S., Stahl, C., Delzon, S., Levionnois, S., Cazal, J., . . . Bonal, D. (2019).
917   Large hydraulic safety margins protect Neotropical canopy rainforest tree species
918   against hydraulic failure during drought. *Annals of Forest Science, 76*(4).
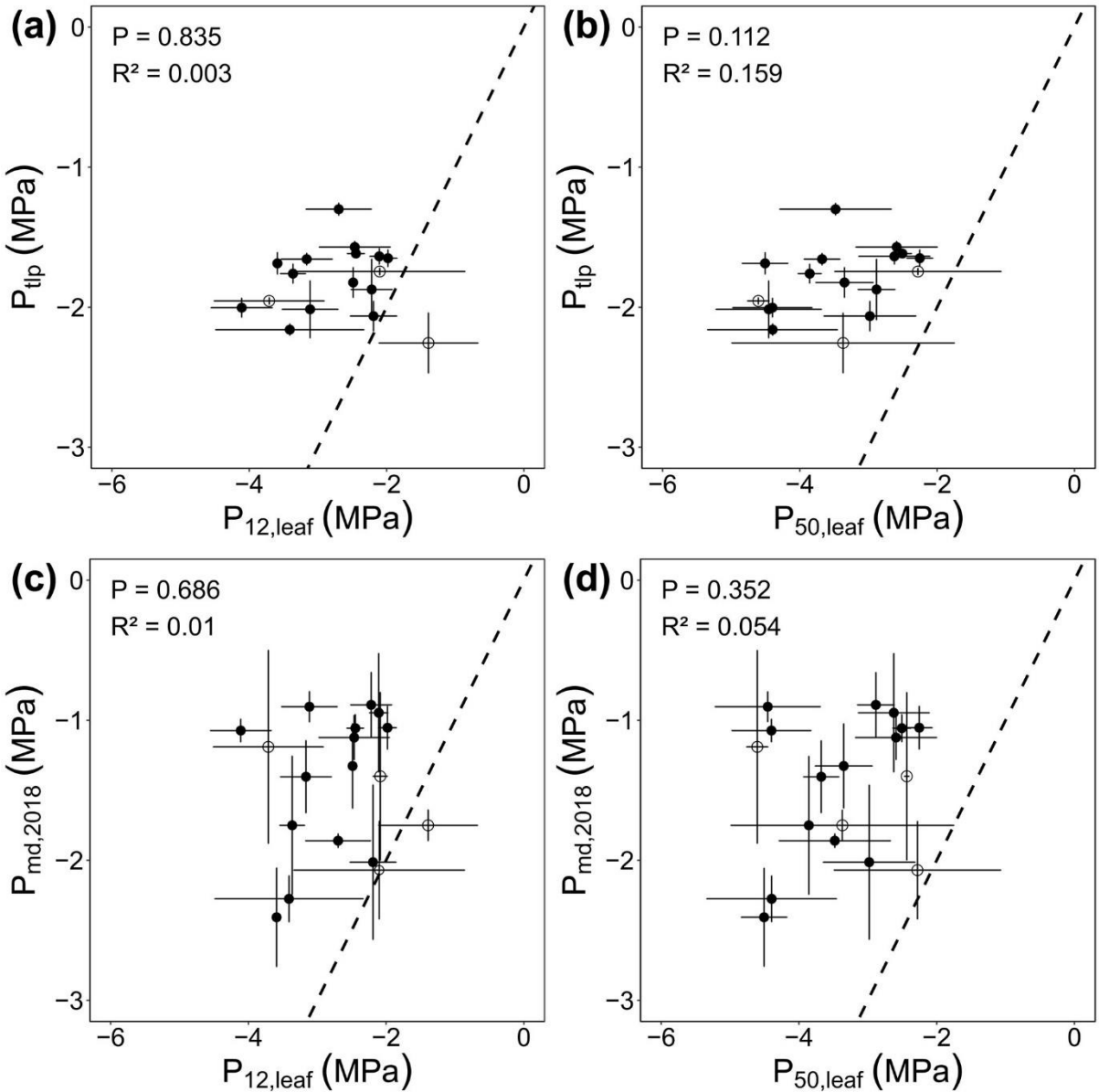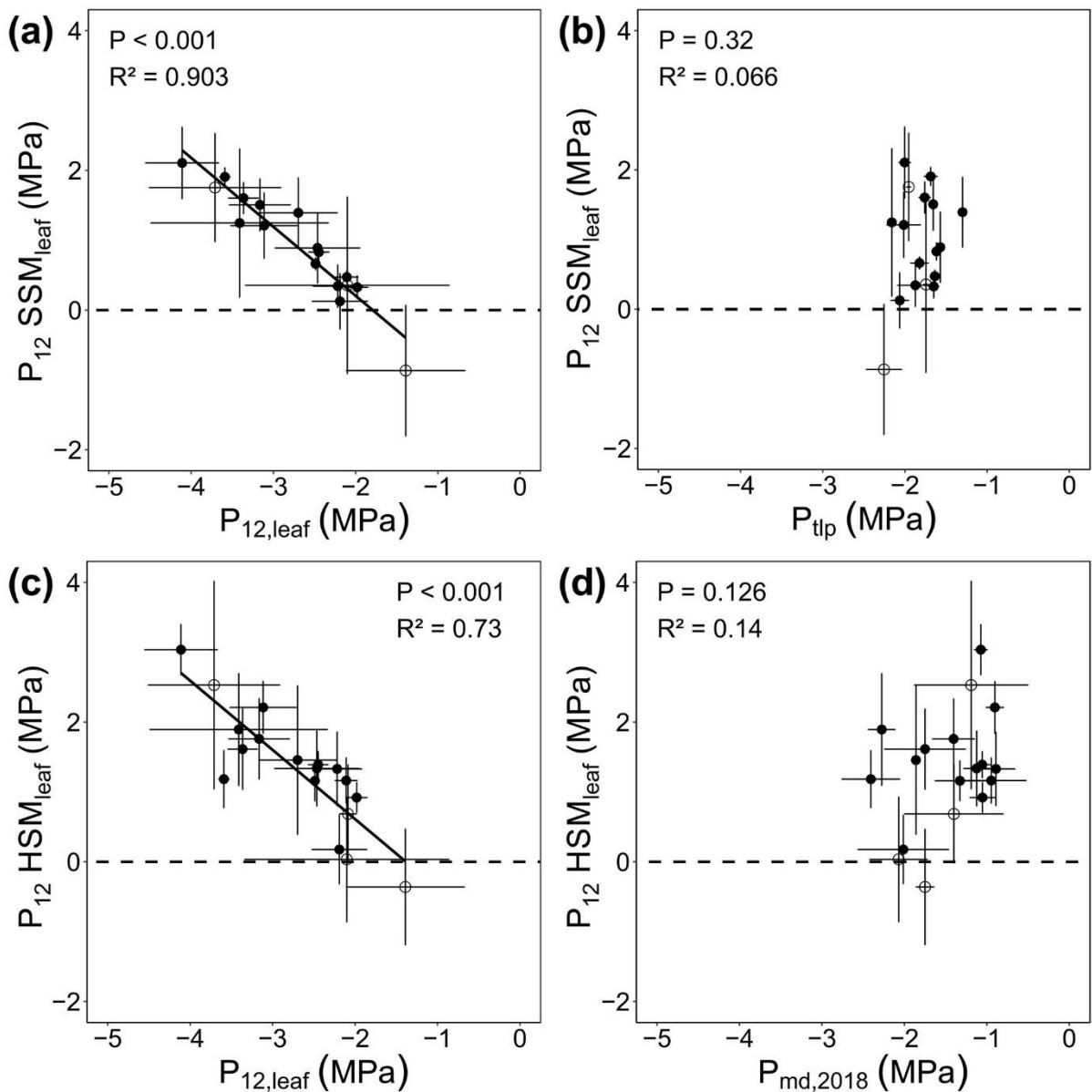919   doi:10.1007/s13595-019-0905-0

920

922

923

Fig. 1. (a) Leaf water potential at turgor loss point (P_{tlp} ; MPa) according to variations in the leaf water potential associated with 12% of leaf xylem embolism ($P_{12,leaf}$, MPa). (b) Leaf water potential at turgor loss point according to the variations in the leaf water potential associated with 50% of leaf xylem embolism ($P_{50,leaf}$, MPa). (c) Leaf water potential at midday (P_{md}, MPa) according to the variations in the leaf water potential associated with 12% of leaf xylem embolism. (d) Leaf water potential at midday according to the variations in the leaf water potential associated with 50% of leaf xylem embolism. One point represents one species (black, n = 3 trees; circle, n = 2 trees). The dashed line represents the 1:1 line. Standard errors, coefficients of determination (R^2) and significance levels (P) are shown.

933

934

Fig. 2. (a) The P_{12} stomatal safety margin (P_{12} SSM$_{leaf}$; $P_{tlp} - P_{12,leaf}$; MPa) according to the variations in the leaf water potential associated with 12% of leaf xylem embolism. (b) The P_{12} SSM$_{leaf}$ according to the variations in the leaf water potential at turgor loss point. (c) The P_{12} hydraulic safety margin (P_{12} HSM$_{leaf}$; $P_{md} - P_{12,leaf}$; MPa) according to the variations in the leaf water potential associated with 12% of leaf xylem embolism. (d) The P_{12} hydraulic safety margin (P_{12} HSM$_{leaf}$; $P_{md} - P_{12,leaf}$; MPa) according to the variations in the leaf water potential at midday. One point represents one species (black, n = 3 trees; circle, n = 2 trees). The horizontal dashed line represents null safety margins. The solid line represents the regression. Standard errors, coefficients of determination (R^2) and significance levels (P) are shown.
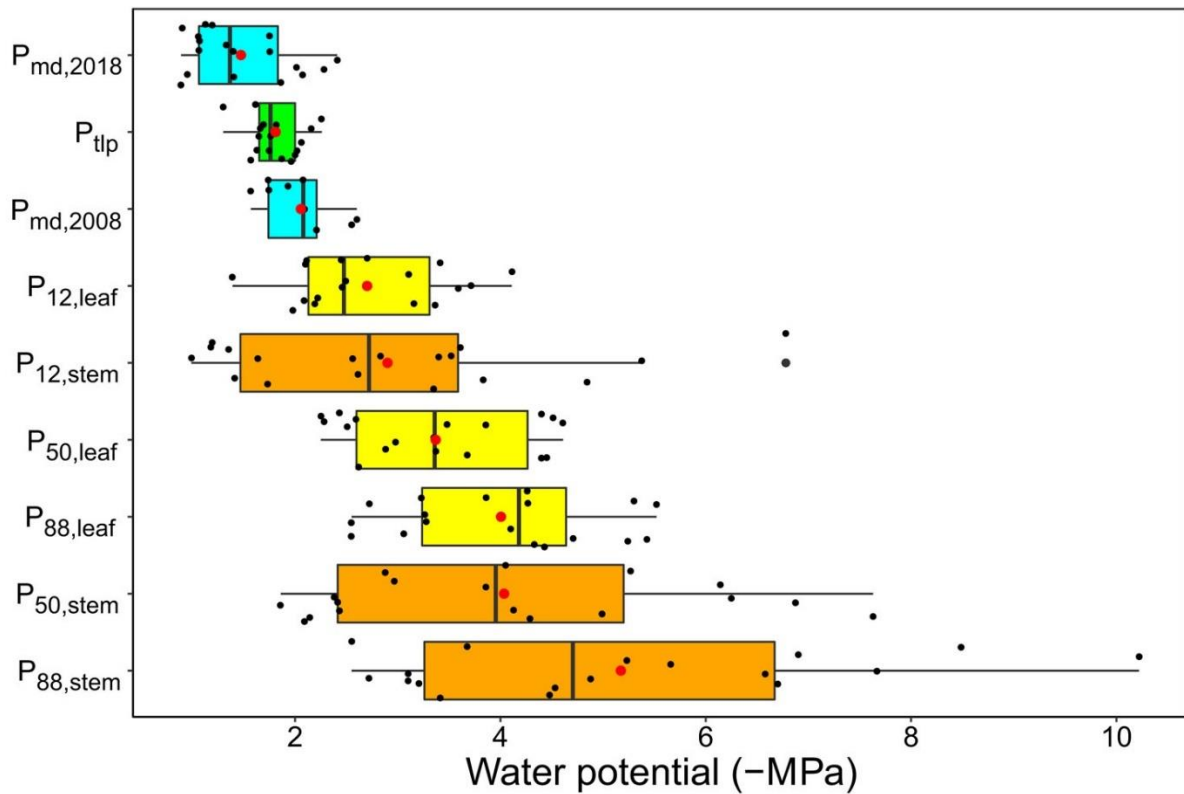
944

32

945

Fig. 3. Sequence of key water potential thresholds during dehydration. Key physiological traits for 18 tropical rainforest tree species are represented: leaf turgor loss point (P_{tlp}; green); the water potential associated with 12, 50 and 88% loss of leaf ($P_{12,leaf}$, $P_{50,leaf}$ and $P_{88,leaf}$; yellow) and stem ($P_{12,stem}$, $P_{50,stem}$ and $P_{88,stem}$; orange) hydraulic conductance; the leaf water potential measured during a normal-intensity dry season in 2018 (P_{md}; blue). Species are represented by black dots. The median is represented by a black bar and the mean is represented by a red dot; the traits are ranked in decreasing order of mean water potential. Black boxes represent the 1st and 3rd quartiles, and error bars represent minimum and maximum values. Mean species values for $P_{12,leaf}$, $P_{50,leaf}$ and $P_{88,leaf}$ were extracted from Levionnois *et al.* (2020), mean species values for P_{tlp}, P_{md}, $P_{12,stem}$, $P_{50,stem}$ and $P_{88,stem}$ were extracted from Ziegler *et al.* (2019).
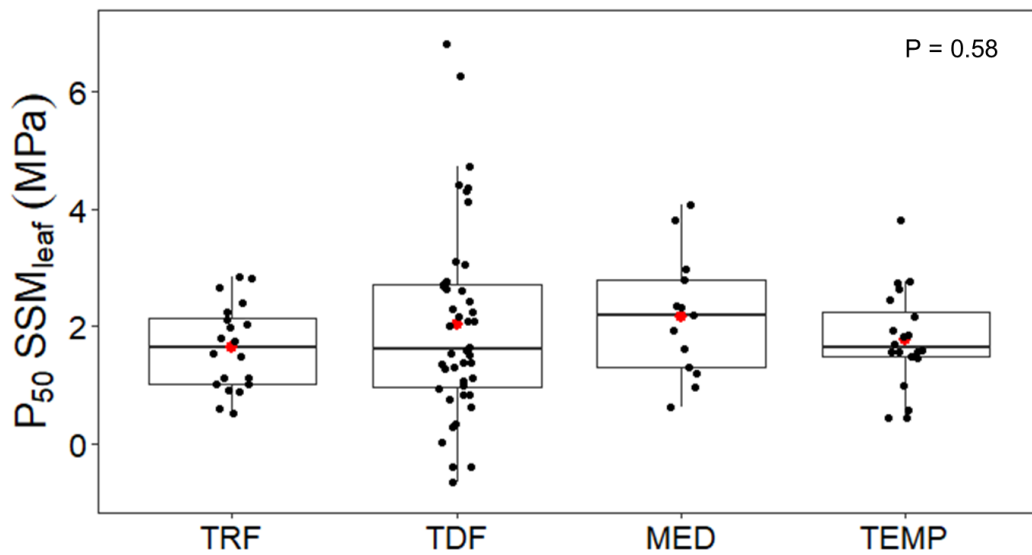
956

957

958 **Fig. 4**. The P_{50} stomatal safety margin (P_{50} SSM_{leaf}; $P_{close} - P_{50,leaf}$; MPa) across major biomes

959 based on a literature survey encompassing 97 species. TRF: tropical rainforests; TDF: tropical

960 dry forests; MED: Mediterranean and dry forests; TEMP: temperate forests. The P-value refers

961 to a Kruskal-Wallis test showing no significant differences across biomes.

Table 1. Species leaf hydraulic parameters. Leaf water potential at turgor loss point (P_{tlp}; MPa), dry season midday leaf water potential measured during the normal-intensity dry season of 2018 (P_{md}; MPa), leaf water potential at 12% ($P_{12,leaf}$; MPa), 50% ($P_{50,leaf}$; MPa) and 88% ($P_{88,leaf}$; MPa) of loss in leaf xylem hydraulic conductance, P_{12} leaf stomatal safety margin (P_{12} SSM_{leaf}; P_{tlp} - $P_{12,leaf}$; MPa), P_{12} leaf hydraulic safety margin (P_{12} HSM_{leaf}; $P_{md,2018}$ - $P_{12,leaf}$; MPa), and the percentage loss in leaf xylem hydraulic conductance in 2018 (PLC_{2018}; %). Mean values ± SE are shown.

Species	n trees	P_{tlp}	P_{md}	$P_{12,leaf}$	$P_{50,leaf}$	$P_{88,leaf}$	P_{12} SSM_{leaf}	P_{12} HSM_{leaf}	PLC_{2018}
Bocoa prouacensis Aubl.	2	-2.0 ± 0.0	-1.2 ± 0.7	-3.7 ± 0.8	-4.6 ± 0.2	-5.4 ± 0.3	1.8 ± 0.8	2.5 ± 1.5	1 ± 1
Chaetocarpus schomburgkianus (Kuntze)	3	-1.6 ± 0.0	-1.1 ± 0.2	-2.5 ± 0.5	-2.6 ± 0.6	-2.7 ± 0.6	0.9 ± 0.5	1.3 ± 0.5	0 ± 0
Chrysophyllum sanguinolentum (Pierre) Baehni	2	-1.7 ± 0.0	-2.1 ± 0.4	-2.1 ± 1.2	-2.3 ± 1.2	-2.5 ± 1.0	0.4 ± 1.3	0.0 ± 0.9	47 ± 47
Dicorynia guianensis Amshoff	3	-1.3 ± 0.0	-1.9 ± 0.0	-2.7 ± 0.5	-3.5 ± 0.8	-4.3 ± 1.1	1.4 ± 0.5	1.5 ± 1.1	25 ± 24
Eperua falcata Aubl.	3	-1.7 ± 0.0	-1.4 ± 0.3	-3.2 ± 0.4	-3.7 ± 0.3	-4.3 ± 0.3	1.5 ± 0.4	1.8 ± 0.6	0 ± 0
Eperua grandiflora (Aubl.) Benth.	3	-2.0 ± 0.1	-1.1 ± 0.1	-4.1 ± 0.4	-4.4 ± 0.6	-4.7 ± 0.7	2.1 ± 0.5	3.0 ± 0.4	0 ± 0
Eschweilera sagotiana Miers	3	-1.7 ± 0.1	-1.1 ± 0.2	-2.0 ± 0.1	-2.3 ± 0.2	-3.1 ± 0.8	0.3 ± 0.2	0.9 ± 0.2	0 ± 0
Goupia glabra Aubl.	3	-1.9 ± 0.2	-0.9 ± 0.2	-2.2 ± 0.3	-2.9 ± 0.3	-3.9 ± 0.4	0.3 ± 0.3	1.3 ± 0.5	2 ± 1
Gustavia hexapetala (Aubl.) Sm.	3	-2.0 ± 0.2	-0.9 ± 0.1	-3.1 ± 0.4	-4.5 ± 0.8	-5.5 ± 0.8	1.2 ± 0.5	2.2 ± 0.4	0 ± 0
Lecythis poiteauii O. Berg	2	-2.3 ± 0.2	-1.8 ± 0.1	-1.4 ± 0.7	-3.4 ± 1.6	-4.1 ± 1.3	-0.9 ± 0.9	-0.4 ± 0.8	28 ± 28
Licania membracea Sagot ex Laness.	3	-1.8 ± 0.1	-1.3 ± 0.3	-2.5 ± 0.0	-3.4 ± 0.4	-4.3 ± 0.9	0.7 ± 0.1	1.2 ± 0.3	1 ± 1
Manilkara bidendata (A. DC.) A. Chev.	3	-2.2 ± 0.0	-2.3 ± 0.2	-3.4 ± 1.1	-4.4 ± 0.9	-5.3 ± 1.1	1.2 ± 1.1	1.9 ± 0.8	2 ± 2
Pradosia cochlearia (Lecomte) T.D. Penn.	3	-1.7 ± 0.1	-2.4 ± 0.4	-3.6 ± 0.1	-4.5 ± 0.3	-5.2 ± 0.5	1.9 ± 0.1	1.2 ± 0.4	1 ± 1

Species	n									
Protium opacum Swart	3	-2.1 ± 0.1	-2.0 ± 0.6	-2.2 ± 0.3	-3.0 ± 0.7	-3.3 ± 0.8	0.1 ± 0.4	0.2 ± 0.5	8 ± 8
Qualea rosea Aubl.	2	-	-1.4 ± 0.6	-2.1 ± 0.1	-2.4 ± 0.0	-3.2 ± 0.4		0.7 ± 0.7	4 ± 4
Symphonia globulifera L.f. sp. 1	3	-1.6 ± 0.0	-1.1 ± 0.1	-2.4 ± 0.1	-2.5 ± 0.1	-2.6 ± 0.1	0.8 ± 0.1	1.4 ± 0.2	0 ± 0
Tachigali melinonii (Harms)						-4.4 ± 0.1			
Zarucchi & Her.	3	-1.8 ± 0.1	-1.8 ± 0.5	-3.4 ± 0.2	-3.9 ± 0.2		1.6 ± 0.2	1.6 ± 0.6	1 ± 1
Virola michelii Heckel	3	-1.6 ± 0.1	-0.9 ± 0.4	-2.1 ± 0.1	-2.6 ± 0.5	-3.3 ± 0.6	0.5 ± 0.1	1.2 ± 0.3	1 ± 1

968

SUPPLEMENTARY MATERIAL

970

971 **Table S2.** Species stem hydraulic parameters. Stem water potential at 12% ($P_{12,stem}$; MPa), 50%

972 ($P_{50,stem}$; MPa) and 88% ($P_{88,stem}$; MPa) loss in stem xylem hydraulic conductivity. Mean values

973 ± SE are shown.

Species	$P_{12,stem}$	$P_{50,stem}$	$P_{88,stem}$
Bocoa prouacensis Aubl.	-3.4 ± 0.5	-4.3 ± 0.2	-5.2 ± 0.3
Chaetocarpus schomburgkianus (Kuntze)	-1.2 ± 0.3	-2.4 ± 0.3	-3.7 ± 0.4
Chrysophyllum sanguinolentum (Pierre) Baehni	-3.6 ± 0.1	-4.1 ± 0.0	-4.5 ± 0.1
Dicorynia guianensis Amshoff	-1.4 ± 0.2	-2.4 ± 0.1	-3.4 ± 0.2
Eperua falcata Aubl.	-2.8 ± 0.8	-3.9 ± 0.6	-4.9 ± 0.6
Eperua grandiflora (Aubl.) Benth.	-5.4 ± 0.3	-6.1 ± 0.1	-6.9 ± 0.2
Eschweilera sagotiana Miers	-2.6 ± 0.1	-2.9 ± 0.1	-3.2 ± 0.2
Goupia glabra Aubl.	-3.4 ± 0.6	-5.0 ± 0.3	-6.6 ± 0.2
Gustavia hexapetala (Aubl.) Sm.	-6.8 ± 0.6	-7.6 ± 0.1	-8.5 ± 0.4
Lecythis poiteauii O. Berg	-1.2 ± 0.2	-2.1 ± 0.3	-3.1 ± 0.6
Licania membracea Sagot ex Laness.	-1.4 ± 0.3	-3.0 ± 0.3	-4.5 ± 0.6
Manilkara bidendata (A. DC.) A. Chev.	-3.5 ± 1.1	-6.9 ± 0.6	-10.2 ± 0.7
Pradosia cochlearia (Lecomte) T.D. Penn.	-4.8 ± 1.0	-6.3 ± 0.5	-7.7 ± 0.2
Protium opacum Swart	-1.7 ± 0.3	-2.4 ± 0.2	-3.1 ± 0.2
Qualea rosea Aubl.	-1.0 ± 0.4	-1.9 ± 0.2	-2.7 ± 0.0
Symphonia globulifera L.f. sp. 1	-1.6 ± 0.2	-2.1 ± 0.1	-2.6 ± 0.0
Tachigali melinonii (Harms) Zarucchi & Her.	-2.6 ± 0.4	-4.1 ± 0.2	-5.7 ± 0.4
Virola michelii Heckel	-3.8 ± 0.6	-5.3 ± 0.3	-6.7 ± 0.2

974

975